C II*/C II ratio in high-redshift DLAs: ISM phase separation drives the observed bimodality of [C II] cooling rates.

S. Balashev[1], K. Telikova[1,2*], P. Noterdaeme[3,4]

[1]Ioffe Institute, Russia
[2]European Southern Observatory, Chile
[3]Institut d'Astrophysique de Paris, France
[4]Franco-Chilean Laboratory for Astronomy, Universidad de Chile, Chile

*ktelikov@eso.org

Abstract

We discuss observations of C II*/C II ratios and cooling rates due to [C II] 158μm emission in high-redshift intervening damped Lyman-α (DLA) systems towards quasars. We show that the observed bimodality in the C II cooling rates actually reflects a bimodality in the C II*/C II–metallicity plane that can be naturally explained by phase segregation of the neutral medium, without invoking differences in star-formation scenarios. Assuming realistic distributions of the physical parameters to calculate the phase diagrams, we also reproduce qualitatively the metallicity dependence of this bimodality. We emphasize that high-redshift DLAs mostly probe low-metallicity gas ($Z \lesssim 0.1 Z_\odot$), where heating is dominated by cosmic rays (and/or turbulence), and not by photoelectric heating. Therefore even if the gas of DLA is predominantly cold (where the cooling is dominated by [C II]), the excitation of C II can be used to derive the cosmic ray ionization rate (and/or turbulent heating), but not the UV field, as was previously considered. Alternatively, if the gas in DLA is predominantly warm, C II*/C II can be used to constrain its number density. https://doi.org/10.1093/mnrasl/slab119

1. Introduction

Carbon is one of the most abundant element in the Universe. Particularly, singly ionized carbon, C II, exists in the ionized as well as in the neutral (cold, CNM, with characteristic temperature $T \lesssim 100\,K$, and warm, WNM, $T \lesssim 10^4\,K$) interstellar medium (ISM). The fine-structure [C II] $\lambda158\,\mu m$ transition from typically collisionally excited $^2P^\circ_{3/2}$ level [9] to the ground state is a key contributor to the cooling of the cold ISM (see e.g. [13]).
Instead of direct [C II] $\lambda158\mu m$ emission, one can estimate the ISM cooling rate l_c (per unit hydrogen atom) in absorption, by measuring the column density $N(\text{C II}^*)$ through the electronic transition at 1335Å [15, 20]:

$$l_c = \frac{N(\text{C II}^*) h\nu_{21} A_{21}}{N(\text{H I})}\ \text{erg s}^{-1}\ \text{H}^{-1}, \qquad (1)$$

where $A_{21} = 2.29 \times 10^{-6}\ \text{s}^{-1}$ is the Einstein coefficient for the spontaneous decay $^2P^\circ_{3/2} \rightarrow {}^2P^\circ_{1/2}$ and $h\nu_{21}$ is the energy of this transition.

2. Observations

Here we focused on the C II excitation in the low-metallicity gas that is typically associated with DLAs. We plot the measurements of [C II] cooling rates in DLAs, compiled from ([21] and references therein) and [6], and our measurements of extremely strong DLA systems (ESDLAs, $N(\text{H I}) \geq 5 \times 10^{21}\ \text{cm}^{-2}$) [18]. Our results tend to support the bimodality in the l_c distribution, previously observed by [21], with the following two groups of DLAs: *high* $\log l_c[\text{erg s}^{-1}\,\text{H}^{-1}] > -27$ and *low* $\log l_c[\text{erg s}^{-1}\,\text{H}^{-1}] \lesssim -27$.

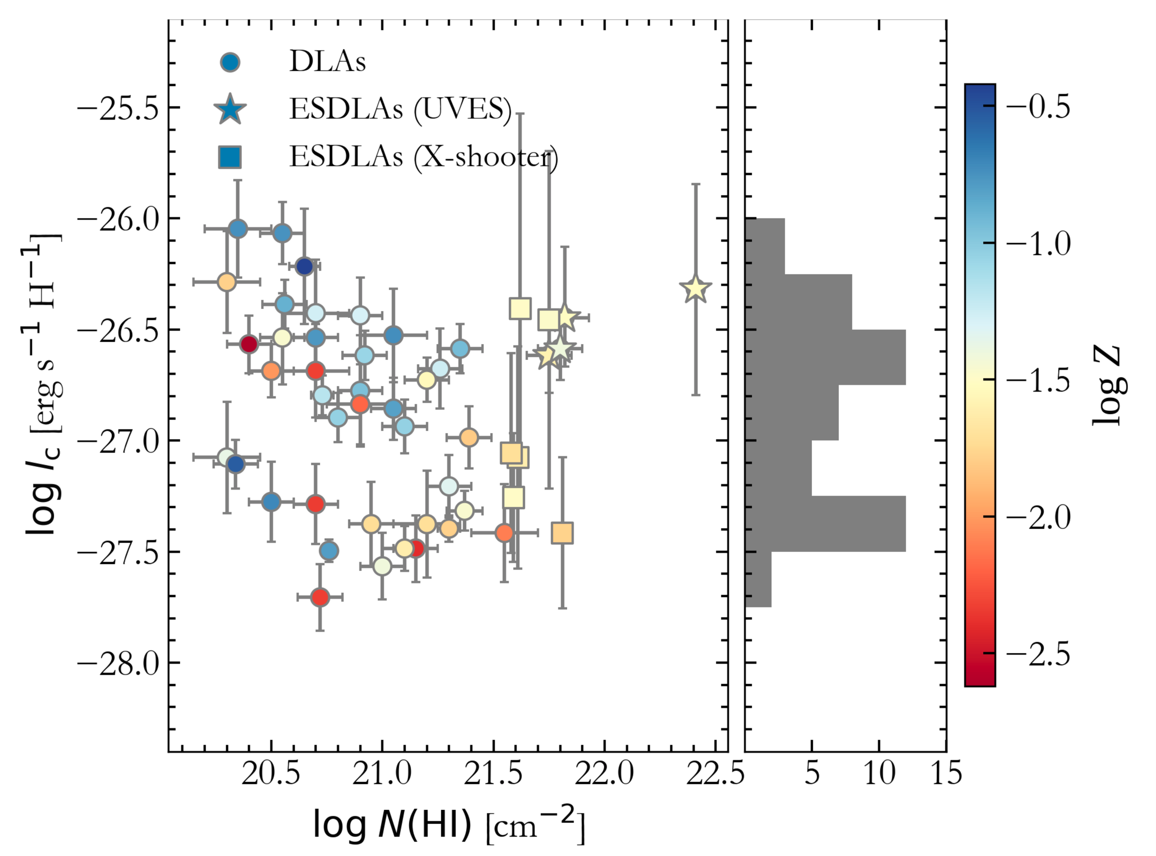

$\log l_c$ vs H I column densities. Colors encode the metallicity[a].

[a]Hereinafter we note metallicity with respect to solar as Z.

3. Interpretation and contradictions

Previous interpretation of the observed bimodality of [C II] cooling rates was proposed in series of papers [20, 19, 21]. Authors assumed that [C II] cooling rate equates photoelectric heating. Since photoelectric heating is scaled with star-formation rates (SFRs), authors interpreted that the bimodality of [C II] cooling rates is due to the bimodality in star-formation regimes in the galaxies associated with the DLAs [21].
However, this interpretation has several open problems:

- typical SFRs from the DLA observations significantly lower, than those, calculated from C II under the above mentioned assumption [8];
- the majority of DLAs probe WNM [17, 10], which is actually predominantly cooled by Lyα emission [14, 5] and not by [C II] emission, which is the main coolant only in CNM;
- DLAs mostly probe low-metallicity gas ($Z \lesssim 0.1$), where heating is dominated by cosmic rays (and/or turbulence), and not by photoelectric heating [3].

Can the bimodality of [C II] cooling rates be explained in alternative way? As seen from Eq. (1) [C II] cooling rate can be expressed via C II*/C II ratio as

$$l_c \propto \frac{N(\text{C II}^*)}{N(\text{H I})} \propto \frac{N(\text{C II}^*)}{N(\text{C II})} \times Z, \qquad (2)$$

where Z is the DLA metallicity. Therefore, to explain the bimodality of l_c one need to explain

- the bimodality of C II*/C II ratio;
- the dependence of C II*/C II ratio on Z.

4. C II*/C II ratio: observations

The dependence of C II*/C II ratio on the metallicity can be investigated in DLAs using measured column densities, as

$$R_C \approx \frac{N(\text{C II}^*)}{N(\text{H I})\,(\text{C/H})_\odot\,\langle Z\rangle_{\text{DLA}}} \equiv \langle R_C\rangle_{\text{DLA}}\,, \qquad (3)$$

where $\langle Z\rangle_{\text{DLA}}$ is the DLA metallicity, averaged over the velocity components and $(\text{C/H})_\odot$ is the solar abundance [1].

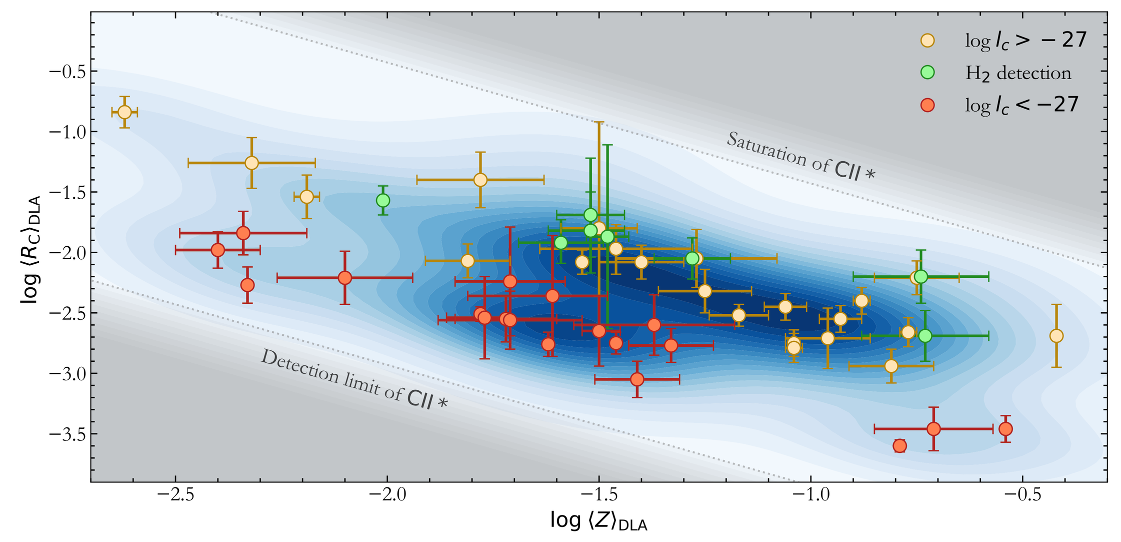

$\langle R_C\rangle_{\text{DLA}}$ as a function of the averaged metallicity in DLAs. The blue contours show the kernel density estimate of the sample. Grey areas correspond to the conditionally defined observational selection of C II*.

One can see that at a given metallicity the R_C values are generally distributed into two groups of relatively *high* and *low* R_C. Since H_2 is always associated with CNM, we also differentiate DLAs, where molecular hydrogen is detected. We found that all these H_2-bearing DLAs are located among the *high* R_C population [17].
Hypothesis: the bimodality in the R_C-Z distribution originates from neutral medium phase separation.

5. ISM phase diagram

We calculated the phase diagram for the neutral ISM assuming thermal balance as was done by [7, 22, 23, 3]. We considered cooling by Lyα [16], C II and O I fine-structure emission, and heating by photo electrons, cosmic rays and turbulence dissipation.

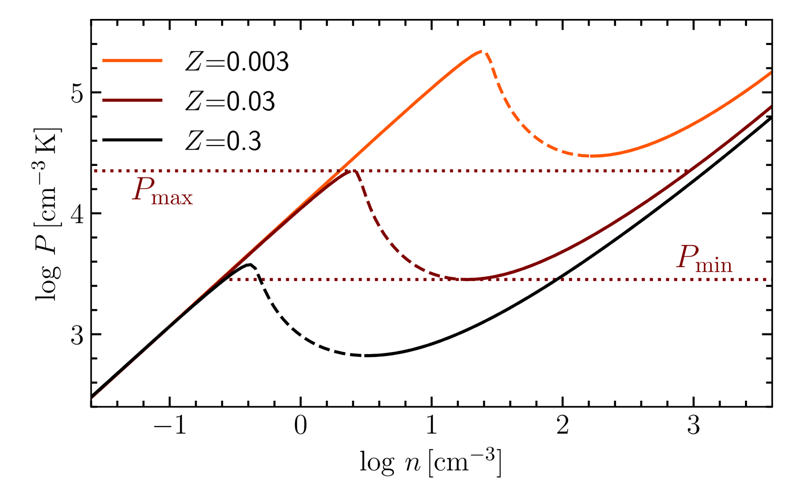

The dependence of phase diagram (pressure vs number density) of the neutral ISM on the metallicity.

An important point here is that the phase diagram of the neutral ISM depends on metallicity [14, 3]: $P_{\min}$ (the minimum pressure for CNM) and $P_{\max}$ (the maximal pressure for WNM) increase with decreasing metallicity.

6. C II*/C II ratio: calculations

Under typical ISM conditions, the C II* level is populated from the ground level by collisions (described by collision rate coefficient C_{12}) and depopulated by spontaneous decay (with the Einstein coefficient A_{21}). Hence the population ratio of $^2P^\circ_{3/2}$ and $^2P^\circ_{1/2}$ levels

$$R_C = \frac{n(\text{C II}^*)}{n(\text{C II})} \approx \frac{C_{12}(T)n}{A_{21}} \qquad (4)$$

depends on the type of the collision partner, the number density, n, and the temperature, T.

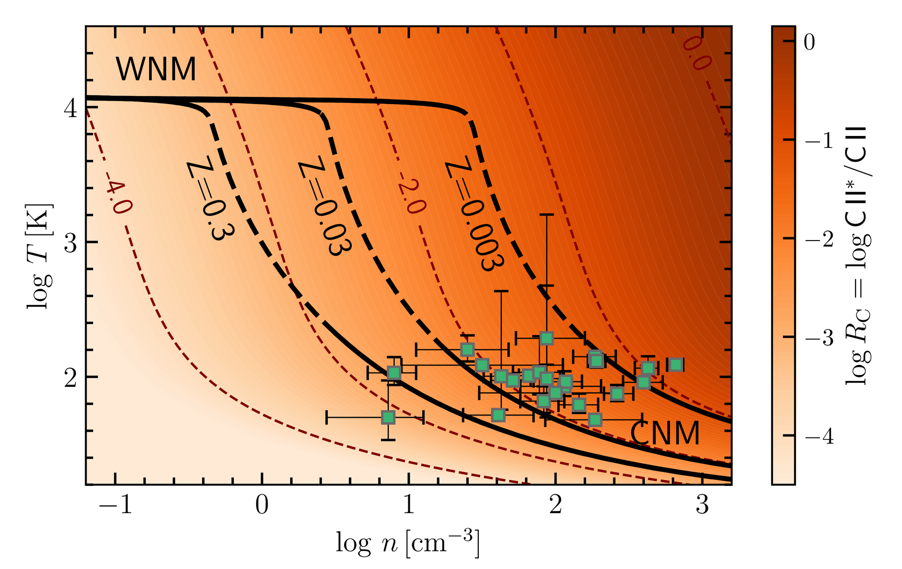

R_C as a function of n and T. The brown curves show the contours of the constant R_C. The black curves correspond to the branches of phase diagrams. Green circles are the measurements in H_2-bearing components of DLAs [11, 2].

7. Results

To test whether CNM and WNM drive the bimodality of R_C-Z distribution, we estimated ranges of R_C in WNM and CNM as a function of metallicity using the calculation of the phase diagram. For each metallicity on a grid varying from 10^{-3} to 1, we generated a distribution of R_C in CNM and WNM by sampling the phase diagrams and characteristic pressures. Additionally, we assumed lognormal distributions with 0.3 dex dispersion and mean of 1 (in Draine units) and $10^{-27}\,\text{erg}\,\text{s}^{-1}$ for the intensity of the UV field and turbulence heating, respectively. We assumed a cosmic ray ionization rate square-law dependence on UV with cosmic ray ionization rate $10^{-16}\,\text{s}^{-1}$ corresponding to Draine field [12]. We also assume the same 0.3 dex dispersion for the dust-to-gas ratio along its quadratic dependence on metallicity. Then for each phase diagram, we estimated the ranges of R_C for CNM and WNM by sampling the pressure uniformly between $P_{\min}$ and $P_{\max}$, estimated for each phase diagram.

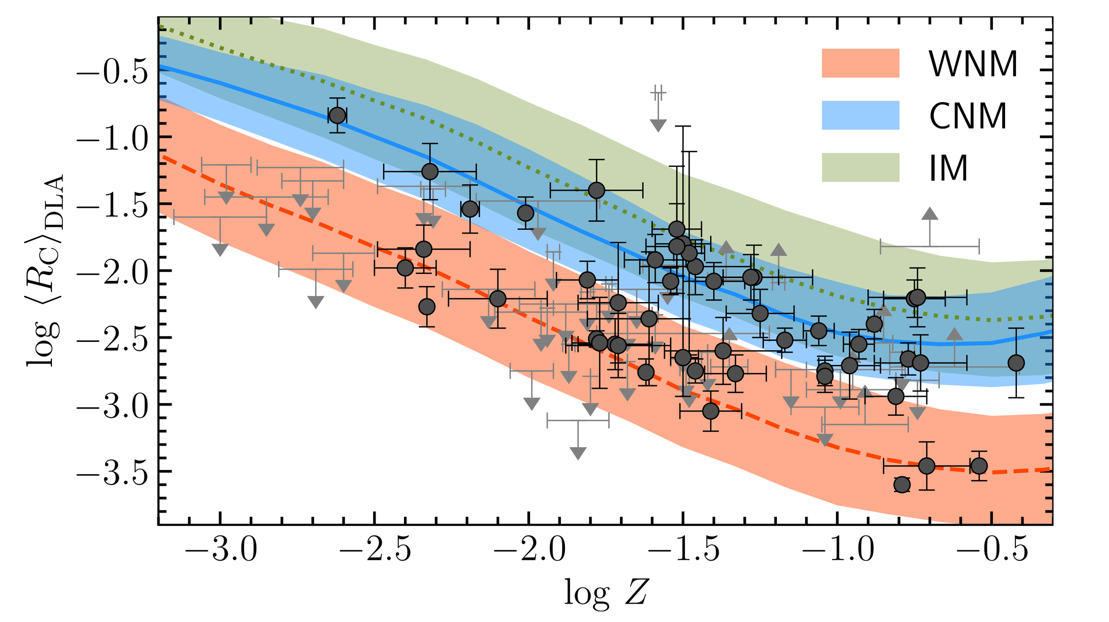

C II*/C II ratio as a function of the metallicity. The black points indicate the observed values in DLAs. The red, blue and olive stripes show the ranges where located 68 percent of the sampled distributions calculated for the WNM, CNM and ionized medium, respectively.

One can see that the phase separation of CNM and WNM explains R_C values measured in DLAs including the general metallicity dependence and the bimodality of R_C distribution at each metallicity. It is important to note that *high* R_C can also arise from ionized medium, which was not taken into account in our model before. We plot the expected R_C in fully ionized gas assuming a temperature of $T_{\text{IM}} = 10^4$ K and the thermal pressure equates neutral phase pressure obtained using aforementioned sampling.

8. Conclusions

1. We showed that the previously reported bimodality of observed **[C II] cooling rates** (l_c) in DLAs is essentially the result of combining two effects:
   - the **phase separation** of the neutral ISM;
   - the **metallicity dependence** of the phase diagram of the neutral ISM.
2. C II*/C II ratio can be used to derive the **cosmic ray ionization rate**, but not UV (and SFR);
3. C II*/C II ratio in the WNM can be used to estimate the **gas number density**.

Acknowledgements

SB and KT are supported by RSF grant 18-12-00301. PN is supported by the French *Agence Nationale de la Recherche* under grant No. 17-CE31-0011-01 ("HIH2").

References

[1] M. Asplund, N. Grevesse, A. J. Sauval, P. Scott., *Ann. Rev. Astron. Astroph.*, 47, 2009.
[2] S. A. Balashev et al., *MNRAS*, 490, 2019.
[3] S. Bialy and A. Sternberg, *Astroph. J.*, 881, 2019.
[4] Renyue Cen, *Astroph. J.*, 748, 2012.
[5] B. T. Draine, Physics of the Interstellar and Intergalactic Medium, 2011.
[6] R. Dutta et al., *MNRAS*, 440, 2014.
[7] G. B. Field, D. W. Goldsmith, H. J. Habing, *Astroph. J. Lett.*, 155, 1969.
[8] M. Fumagalli et al., *MNRAS*, 446, 2015.
[9] P. F. Goldsmith, W. D. Langer, J. L. Pineda, T. Velusamy, *Astroph. J. Suppl.*, 203, 2012.
[10] N. Kanekar et al., *MNRAS*, 438, 2014.
[11] V. V. Klimenko and S. A. Balashev, *MNRAS*, 498, 2020.
[12] D. N. Kosenko et al., *MNRAS*, 505, 2021.
[13] G. Lagache, M. Cousin, M. Chatzikos, *A&A*, 609, 2018.
[14] H. Liszt, *A&A*, 389, 2002.
[15] S. R. Pottasch, P. R. Wesselius, R. J. van Duinen, *A&A*, 74, 1979.
[16] L. Spitzer, Physical processes in the interstellar medium, 1978.
[17] R. Srianand et al., *MNRAS*, 362, 2005.
[18] K. N. Telikova et al., *MNRAS, 510*, 2022.
[19] A. M. Wolfe, E. Gawiser, J. X. Prochaska, *Ann. Rev. Astron. Astroph.*, 43, 2005.
[20] A. M. Wolfe, J. X. Prochaska, E. Gawiser, *Astroph. J.*, 593, 2003.
[21] A. M. Wolfe, J. X. Prochaska, R. A. Jorgenson, M. Rafelski, *Astroph. J.*, 681, 2008.
[22] M. G. Wolfire et al., *Astroph. J.*, 443, 1995.
[23] M. G. Wolfire, C. F. McKee, D. Hollenbach, A. G. G. M. Tielens, *Astroph. J.*, 587, 2003.